

Supplemental Materials



APPENDIX A THE SPACE-FILLING CURVE TECHNIQUE

The main challenge of extending the EMD into higher dimensional signals arises in the construction of the upper and lower envelopes. Though the EMD algorithm does not require the envelopes to be strictly precise and does not specify how to generate data envelopes, it is still not easy to find a practical way concerning speed requirements in computer graphics. Most of the methods to calculate envelopes in 1D or 2D, such as radial function method in [1] and [2], interpolation based on Delaunay triangulation as in [3], combination of separate 1D EMD for each dimension as in [4], suffer problems of either high-cost, low-automation or losing high-dimensional connection. From these concerns we propose to use the space-filling curve technique. Basically the space-filling curve technique is a method to flatten 3D data into 1D. An n -dimensional space-filling curve is a curve that can fill the whole n -dimensional domain, such that moving along the curve gives a mapping from the high-dimensional space to 1D. The space filling curve technique was first introduced into 3D fluid simulation in [5]. In the case of 3D grid, this means an continuous indexing of the grid cells. The EMD operations can be performed on the flattened 1D data, giving envelopes of the 1D indexing array. It is easy to verify that the obtained envelopes are still envelopes of the original 3D grid data if mapped back. Such envelopes are not the optimal choice in terms of accuracy, but the effectiveness of EMD is not affected as long as the envelope is valid, for the reduced accuracy mainly affects the time to converge.

Some examples of the EMD results using the space-filling curve technique are listed below. For comparison, we implemented the RBF-EMD method used by [1], which uses radial basis functions (RBF) for upper and lower envelope calculation in 2D space and was reviewed by [6] as the benchmark reference for 2D EMD decomposition. The reference results here serve to give an intuitive observation of the multi-level structures of the flow fields.

Fig. 1 is a 2D decomposition example. A double-swirl flow field is decomposed into two levels of flow-field structures with relatively high and low frequency ranges. Fig. 1(a) shows the original flow field, the results using the space-filling curve technique (based

on quadric Koch curve) are shown Figs. 1(b) and 1(c) for higher- and lower- frequencies respectively, and the corresponding results using the RBF-EMD method are shown in Figs. 1(d) and 1(e). The decomposition results of the Koch curve largely catch the structures of the flow field, but there are some frequency overlaps, leading to a “half swirl” like feature in the left part of Fig. 1(b). It is interesting to note that for both higher- and lower- frequencies the RBF-EMD method gives relatively large velocity values in the top-left corner. This may be due to superposition of the smooth radial basis functions (the top-left corner is far from any RBF kernel center). The method using quadric Koch curve does not introduce these artificial velocities.

Fig. 2 is a 3D decomposition example. Unfortunately the RBF-EMD method cannot directly apply to 3D cases, so we examine the performance of the space-filling curve technique through a case that is theoretically trivial and intuitive. Specifically, an artificial cylindrical swirl of $128 \times 128 \times 128$ size is decomposed. Along the vertical direction (i.e. the z -axis), the velocity component is always zero; within the horizontal plane (i.e. the xy -plane), the velocity magnitudes of the swirl is proportional to the distance from the central z -axis. The 63rd slice (xy -plane) of the original flow field is shown in Fig. 2(a). This trivial flow field has only one scale of fluid motion, i.e. the swirl rotating at a constant speed. Therefore, an ideal multidimensional-EMD method should stop the iteration immediately and leave all velocity magnitudes into the residual. We apply the 3D EMD method with the 3D Hilbert curve proposed in the main text and extract $9 + 1$ components as the result. It is found that the first 9 components all have near-zero values and for demonstration, the 63rd slices for the 9th and the 8th components are shown in Figs. 2(c) and 2(d). The residual is shown in Fig. 2(b), which as anticipated fully recovers the single scale swirl. In this example, the error caused by sampling along the space-filling curve is generally more than an order of magnitude smaller than the total velocity.

REFERENCES

- [1] J. Nunes, Y. Bouaoune, E. Delechelle, O. Niang, and P. Bunel, “Image analysis by bidimensional empirical mode decomposition,” *IMAGE AND VISION COMPUTING*, vol. 21, no. 12, pp. 1019–1026, NOV 1 2003.

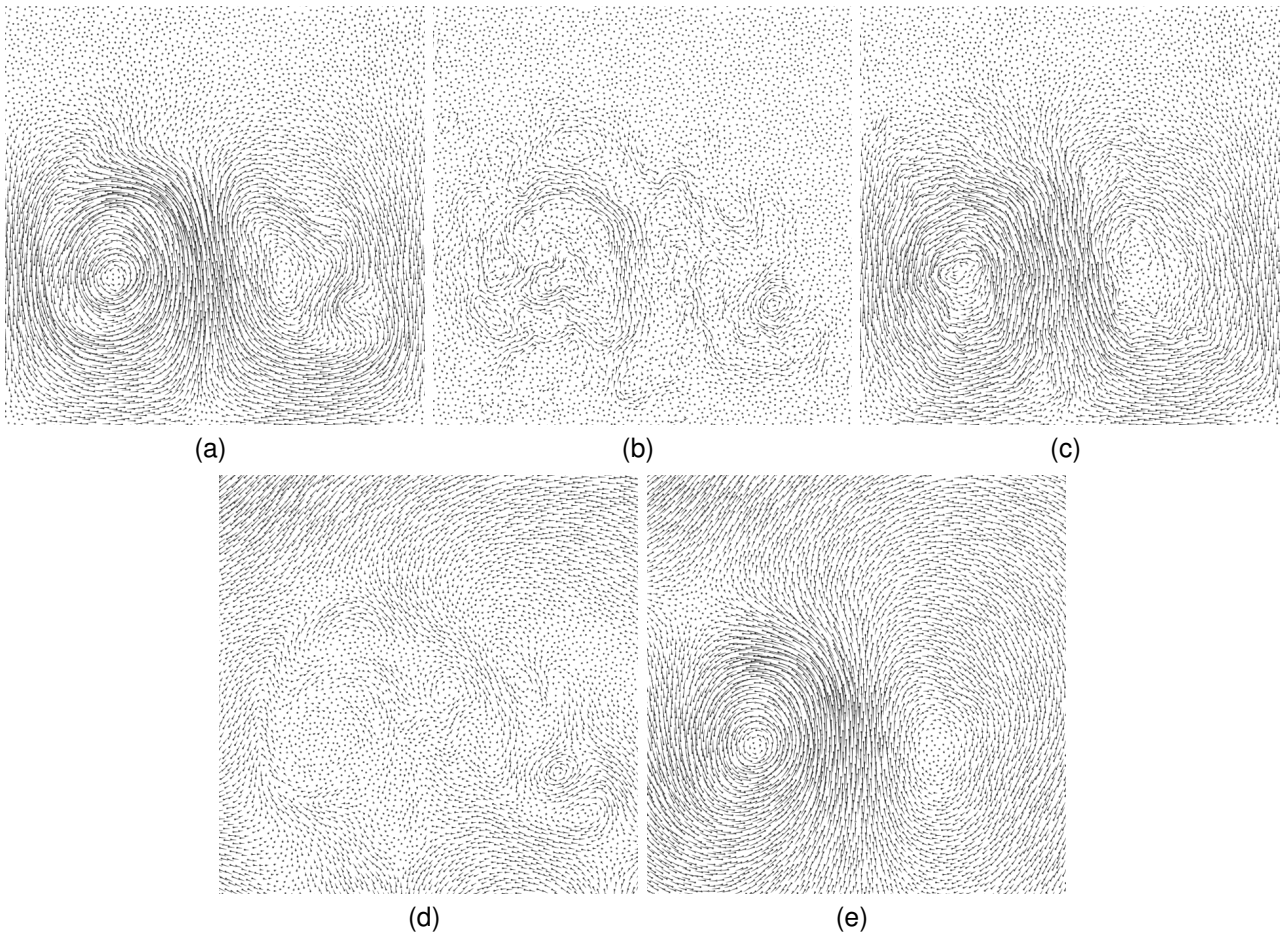


Fig. 1. 2D decomposition example. (a) the original; (b) the higher-frequency decomposition result using the space-filling curve; (c) the lower-frequency decomposition result using the space-filling curve; (d) the higher-frequency decomposition result using the RBF-EMD method; (e) the lower-frequency decomposition result using the RBF-EMD method.

- [2] K. Subr, C. Soler, and F. Durand, "Edge-preserving multiscale image decomposition based on local extrema," *ACM Trans. Graph.*, vol. 28, pp. 147:1–147:9, December 2009. [Online]. Available: <http://doi.acm.org/10.1145/1618452.1618493>
- [3] C. Damerval, S. Meignen, and V. Perrier, "A fast algorithm for bidimensional EMD," *IEEE SIGNAL PROCESSING LETTERS*, vol. 12, no. 10, pp. 701–704, OCT 2005.
- [4] Z. Liu and S. Peng, "Boundary Processing of bidimensional EMD using texture synthesis," *IEEE Signal Processing Letters*, vol. 12, no. 1, pp. 33–6, January 2005.
- [5] Y. Gao, C.-F. Li, B. Ren, and S.-M. Hu, "View-dependent multiscale fluid simulation," *IEEE Transactions on Visualization and Computer Graphics*, vol. 19, no. 2, pp. 178–188, 2013.
- [6] Z. Wu, N. E. Huang, and X. Chen, "The multi-dimensional ensemble empirical mode decomposition method," *Advances in Adaptive Data Analysis*, pp. 339–372, 2009.

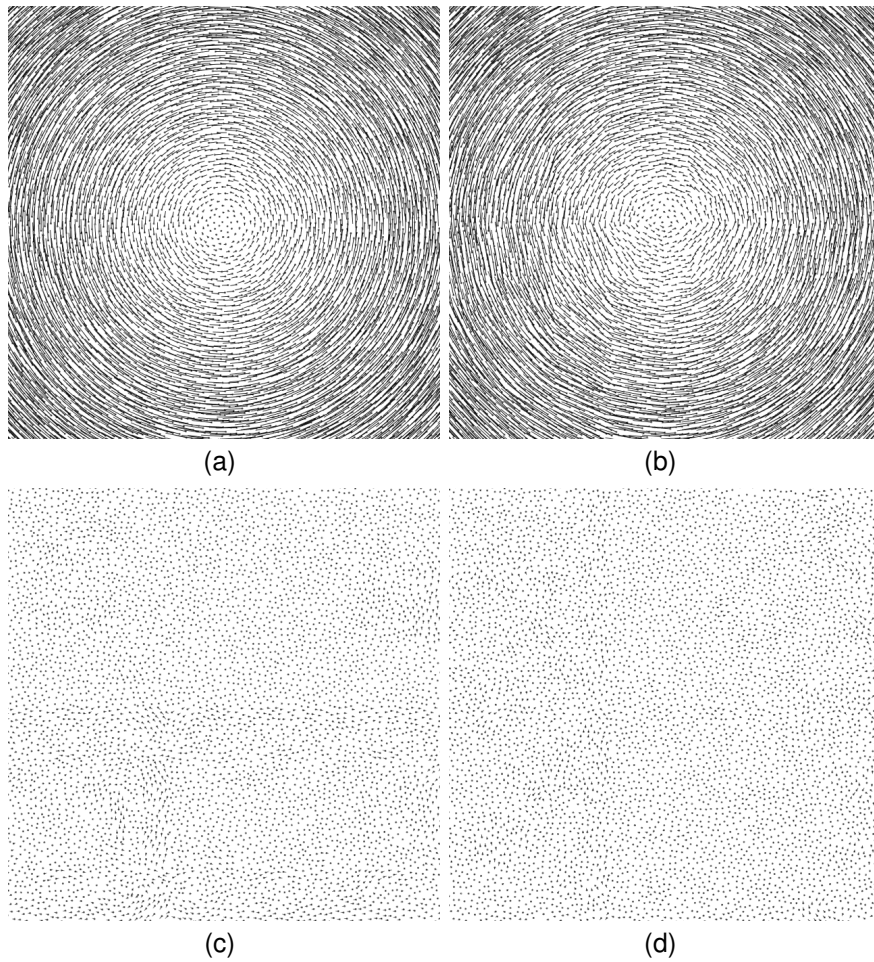


Fig. 2. 3D decomposition example (top view of a cylindrical swirl). (a) the original; (b) the residual; (c) the 9th component; (d) the 8th component.